



Proposing Formula-Based Design Method for RC Columns and Uniformly Reinforced Shear Walls

Jalil Shafaei^{1,*}; Rasoul Eskandari²

¹ Corresponding Author, Assistant Professor, Faculty of Civil Engineering, Shahrood University of Technology, Shahrood, Semnan, Iran

² Graduate student, Faculty of Civil Engineering, Shahrood University of Technology, Shahrood, Semnan, Iran

ABSTRACT: In recent decades, Reinforced Concrete (RC) structures have been impressively grown in construction and research fields. The RC Column is a major component of RC building structures. Design of RC columns and shear walls is an iterative and time-consuming process which often carried out using P-M interaction diagrams (PMID) in hand calculations. In this paper, with a different attitude on conventional approaches and using curve and surface fitting techniques, a simple Formula-based Design (FbD) method for design of RC column and Uniformly Reinforced Shear Wall (URSW) is proposed by which the longitudinal reinforcement area to section gross area ratio can be determined according to sectional details and other assumptions. This proposed dimension-independent method is compatible with any applied axial loads and bending moments, and decreases the complexity and time of design iterations in hand calculations of design and analysis process. Also, these well-organized formulas are useful for direct modeling of standard shapes of column in different research fields. Further, a procedure for determining the strength reduction factor is provided according to ACI 318 Code requirements. The validity and accuracy of the proposed FbD method is investigated by comparing with conventional hand calculation methods, and by several assessments, which shows that this method is suitable for the faster hand design of RC columns and URSWs with satisfying accuracy.

Review History:

Received: 2019-02-02

Revised: 2019-04-24

Accepted: 2019-04-26

Available Online: 2019-04-27

Keywords:

Reinforced Concrete structures

RC Columns

Shear Walls

P-M Interaction Diagrams

Curve fitting

Formula-based Design (FbD) method

1- INTRODUCTION

By assuming a series of strain distributions and computing the related values of axial and bending capacities in each distribution, Short Column Interaction Diagrams are derived. Using such diagrams along principal axes of symmetry is common and accepted approach for the design of RC under combined axial load and bending moments [1]. Interaction diagrams for columns are generally computed by assuming a series of strain distributions, each corresponding to a particular point on the interaction diagram, and computing the corresponding values of P and M [1].

The general procedure of designing RC column and URSW is defined as a series of iteration in which a cross section is assumed and the corresponding interaction diagrams are used. When the assumed cross section satisfies the factored load and moment, the iteration terminates. This is not necessarily the exact fitted solution. For achieving a cross section closer to the fitted solution, the iteration has to continue. Any attempt of development in this iterative procedure without adding more computational cost and complexity can play an important role in structural design science.

This paper proposed an accurate, efficient simple Formula-based Design (FbD) method which does not need computer

*Corresponding author's email: jshafaei@shahroodut.ac.ir

programs and solving the complicated equations. Using the proposed procedure, the longitudinal reinforcement area to section gross area ratio is directly derived. In other words, the percentage of longitudinal reinforcement in cross section can be directly calculated based on the presented formula. Since the strength factor is used in the design procedure, a procedure for determining this factor is proposed.

Like prepared common design diagrams, some values are provided for each case as specific options, including cross section shape and arrangement, compression strength of concrete (f'_c), yielding strength of steel (f_y) and parameter γ , for designing columns and URSWs.

2- PREVIOUS WORKS ON RC COLUMN ANALYSIS AND DESIGN

Several studies were carried out in an attempt to overcome the problems and difficulties of traditional methods and techniques of reinforced concrete column design. Most of the used methods proposed by concrete standards and concrete handbook is graphical technique such as using interaction diagrams along principal axes of symmetry. A method called reciprocal interaction equation which used in ACI 318 commentary was developed by Bresler [2]. many columns in an actual building, are subject simultaneously to bending moments about both major axes in addition to an



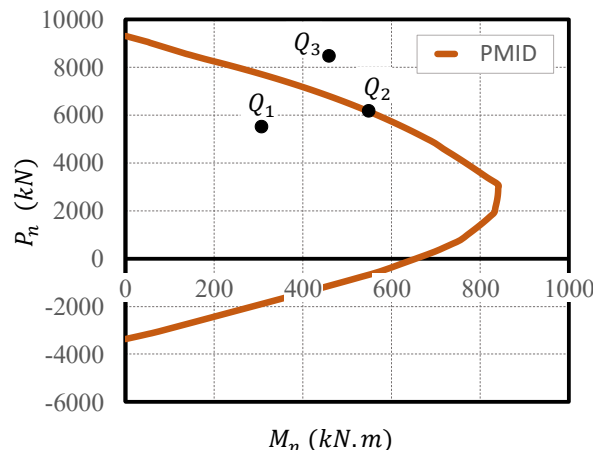


Fig. 1. PMID for case with $h = b = 50\text{cm}$, $f'_c = 210 \text{ kg/cm}^2$, $f_y = 3000 \text{ kg/cm}^2$, $\gamma = 0.8$ and five #8 bars at each side of cross section, and three possible position for point $Q (P_u, M_u)$

axial load. This type of loading is called “biaxial loading” or “biaxial bending”. The ultimate strength of biaxially loaded reinforced concrete columns has been investigated by Chu and Pabarcus [3]. An equivalent compression stress block for simulation of nonlinear behavior of concrete in compression zone was introduced by Whitney [4]. Acceptable strength for biaxial bending accompanying compression loading has been investigated by Hsu and Mirza [5]. A design help relationship considering the nominal axial load and balanced axial load ratio was proposed by Hsu [6]. Design recommendation for columns subjected to biaxial bending in addition to an axial load was developed Fleming and Werner [7].

Also, some researchers studied different shapes of the reinforced concrete column section and reported their design recommendations. Design aids for L-Shaped reinforced concrete column sections were developed by Marin [8]. Theoretical and experimental results and design recommendations for biaxially loaded L-Shaped reinforced concrete column sections presented by Hsu [9]. Hsu [10] reported also design recommendations for T-Shaped column section under biaxial bending and axial compression.

Using computer technology developments made researchers able to step into the different direction of RC column researches. A program for column analysis and calculating stress in steel bars and concrete with a programmable calculator was developed by Dinsmore [11]. Brondum-Nielsen [12] and Yen [13] presented techniques for calculating nominal flexural capacity strength of cracked arbitrary concrete sections under axial load combined with biaxial bending. Bonet et al. [14] proposed an analytical approach for calculating interaction moment-axial failure surfaces in rectangular reinforced concrete column cross sections with symmetrical reinforcement. Paultre et al. [15] presented new equations for design of confinement reinforcement for rectangular and circular columns. An interactive spreadsheet for concrete sections analysis under biaxial bending was developed by Barzegar and Erasito [16].

The behavior of reinforced concrete column under biaxial cyclic loading was studied by Rodrigues et al. [17]. Zenon et al. [18] introduced a method for designing reinforced concrete short columns with hoop ties using the optimization method. A revision to the strength reduction factor for axially loaded concrete columns was proposed by Lequesne-Pincheira [19]. Wang-Hong [20] used the reciprocal load technique for estimating the axial-moment capacity of reinforced concrete columns with high strength concrete. Ochoa [21] developed a computer algorithm for calculating biaxial axial-moment interaction diagrams for short RC column with arbitrary cross section. Cedolin et al. [22] proposed an approximate analytical solution for calculating the failure envelope curve of rectangular reinforced concrete columns. Mahamid and Houshiar [23] proposed a direct technique and design diagrams for RC elements such as columns and shear walls. Mentioned researchers make an effort to provide straightforward design equations or design recommendations.

3- PROBLEM STATEMENT AND RESEARCH SIGNIFICANCE

As mentioned, design of RC short column and URSW is an iterative and time-consuming process. By knowing the factored load (P_u) and moment (M_u) which are applied to column or URSW, there are two common possible approaches in hand calculations.

In the first approach, by guessing whole section including area of section and size and arrangement of bars, the PMID of guessed section can be plotted in analysis stage, which has to be multiplied by strength reduction factor ϕ . In control stage, it is checked whether the factored load and moment point $Q (P_u, M_u)$ falls into the derived diagram. Fig. 1 shows PMID for a square cross section with $h = b = 50\text{cm}$, $f'_c = 210 \text{ kg/cm}^2$, $f_y = 3000 \text{ kg/cm}^2$, $\gamma = 0.8$ and five #8 bars at each side of cross section, and three possible positions for Q . Every position means different state of satisfaction. Q_1 completely falls into the diagram, which means that the assumed section

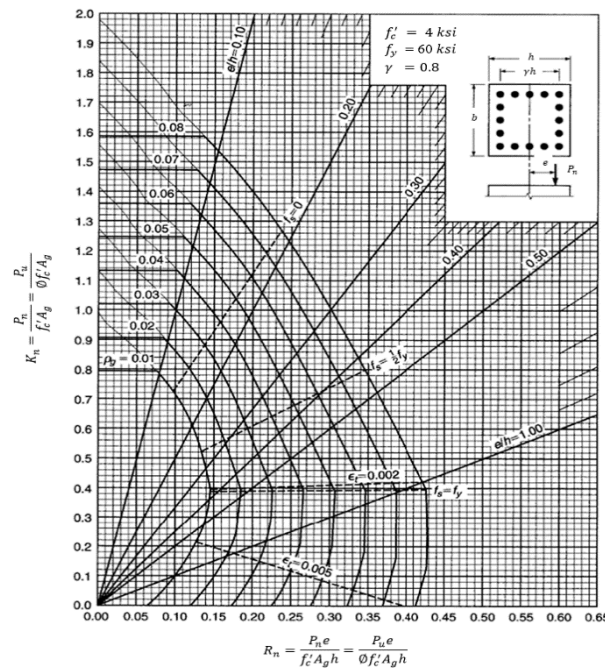


Fig. 2. $K_n \cdot R_n$ design diagram for rectangular column with $f'_c = 4 \text{ ksi}$ (28MPa), $f_y = 60 \text{ ksi}$ (420MPa), $\gamma = 0.8$ and 5 bars at each side of cross section [24]

for column or URSW is suitable for satisfying the applied P_u and M_u , but in uneconomical manner. Q_2 is exactly on the curve, which means that guessed section is satisfactory, and the section is the fitted solution for the column or URSW. Q_3 which appears out of the diagram shows that the guessed section is not appropriate for the applied load and moment, which means that the failure is occurred for the column. Then, a new section should be assumed, and this process will repeat until Q_1 or Q_2 position happens. This trial-and-error procedure can cause time-consuming iterations which is considered as a problem in hand calculations.

In the second approach, by assuming the dimensions of section and calculating the value of eccentricity e , design diagrams provided by codes and references for specific f'_c , f_y , bars arrangement and γ can be used to determine the reinforcement area to section gross area ratio ρ . Fig. 2 illustrates the design interaction diagram with *ksi* unit for strength parameters and *inch* unit for geometric parameters, for rectangular cross section with $f'_c = 4 \text{ ksi}$, $f_y = 60 \text{ ksi}$, $\gamma = 0.8$ [24]. The use of such diagrams can be confusing, and also decrease the accuracy of design procedure in hand calculations. Load capacity tables, 3D interaction diagrams and using computer programs are the other accepted procedures for RC column design [23].

The value ρ derived from proposed formula is the exact demanded percentage of longitudinal reinforcement in cross section. Due to being formula-based and universality, this simplified method is distinguished among the others.

4- Used Techniques

To achieve the purpose of this research, the modeling

of the column is performed in MATLAB according to the distribution theory provided by ACI 318-14 building code requirement [25]. Curve Fitting Application in MATLAB also has been used in the determining the presented formulas.

4.1. Assumptions and Modeling Criteria

ACI design assumptions and formulation basis considered in the modeling are detailed in the following subsections (see Fig. 3). It should be noted that for deriving the PMID of a giving cross section, the procedure contained the following four stages is performed for different values of c which is the distance from the fiber of maximum compressive strain to the neutral axis.

4.1.1. General Assumptions

It is assumed that the geometric proportion is established between strains in the reinforcing bars and concrete. Also, the reinforcement is considered to be stress-perfect plastic. The allowable interval for percentage of reinforcement in cross section is suggested to be $1\% \leq \rho \leq 8\%$.

4.1.2. Strain and Stress Distribution Stage

Maximum strain at the extreme concrete compression fiber is $\epsilon_{cu} = 0.003$. The strain in the i th row of bars is defined as:

$$\epsilon_{si} = \left[\frac{c - d_i}{c} \epsilon_{cu} \right] \quad (1)$$

Where d_i is the distance between i th row and fiber of maximum compressive strain. It should be noted that if the

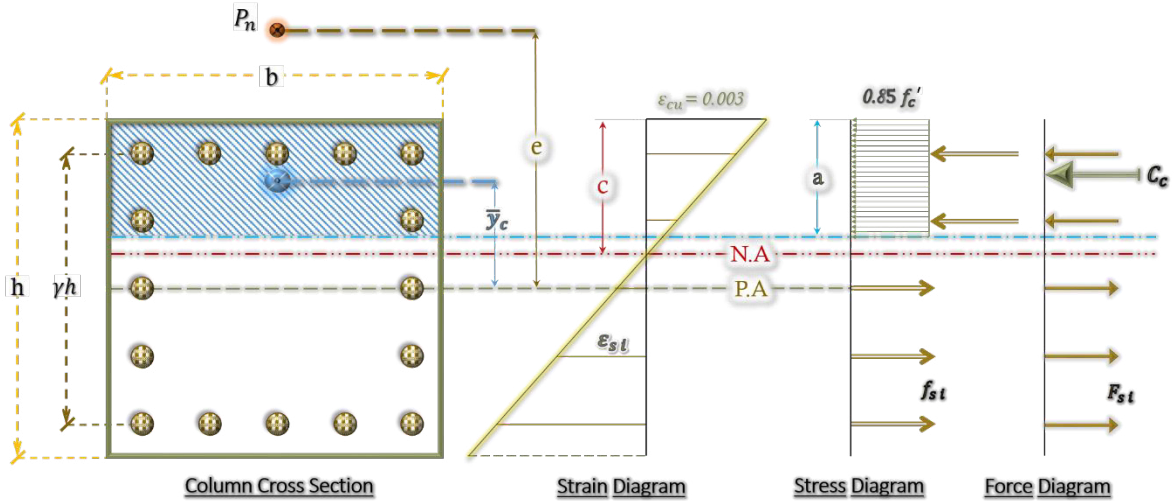


Fig. 3. Visual behavior of column with typical cross section under eccentric load (The hatched zone is compression zone and the other side is tension zone)

i th row of bars is settled at the compression zone, then $\varepsilon_{s,i}$ will be a positive value, and if the i th row of bars is settled at the tension zone, then $\varepsilon_{s,i}$ will be a negative value.

Since the tensile strength of concrete in flexure is approximately 10 to 15 percent of the compressive strength, the tensile strength of concrete is neglected. Also, using stress block to replace detailed approximation of concrete stress distribution is used allowable. In the defined block, uniformly distributed concrete stress of $0.85f'_c$ is assumed over an equivalent compressive region bounded by edge of cross section and a straight line parallel to the neutral axis located a distance $a = \beta_1 c$ from fiber of maximum compressive strain. The value of coefficient β_1 is suggested to be equal to 0.85 for $25 \leq f'_c \leq 40 \text{ MPa}$ by ACI. The following equations can be used to calculate the created stress in the i th row of bars at tension zone, the i th row of bars at compression zone, respectively,

$$\begin{cases} \text{if } |\varepsilon_{s,i}| < \varepsilon_{su} \rightarrow f_{s,i} = \varepsilon_{s,i} E_s \\ \text{if } |\varepsilon_{s,i}| \geq \varepsilon_{su} \rightarrow f_{s,i} = f_y \end{cases} \quad (2)$$

where $E_s = 2 \times 10^5 \text{ MPa}$ is elastic modulus of steel.

4.1.3. Force Stage

After determining stress distribution, and considering $A_{s,i}$ as the total area of i th row of bars and A_c as the area of concrete in compression zone, the force in each component of cross section is calculated as:

$$F_{s,i} = f_{s,i} A_{s,i} \quad (3)$$

$$C_c = 0.85 f'_c A_c \quad (4)$$

where $F_{s,i}$ and C_c are force in i th row of bars and

compressive force in concrete, respectively.

In the square cross sections, the area of compressive concrete is determined as:

$$A_c = a \times b \quad (5)$$

where b is the width of cross section. In the circular cross sections, this parameter specified as:

$$A_c = \frac{h_c}{4} (\theta - \sin\theta \cos\theta) \quad (6)$$

where θ in radian is

$$\begin{cases} \theta = \cos^{-1} \left(1 - \frac{2a}{h_c} \right) & \text{for } a \leq \frac{h}{2} \\ \theta = 180^\circ - \cos^{-1} \left(\frac{2a}{h_c} - 1 \right) & \text{for } a > \frac{h}{2} \end{cases} \quad (7)$$

and h_c is the diameter of circular cross section.

4.1.4. Capacity Evaluation Stage

Finally, the process of calculating the nominal compressive axial capacity P_n , and nominal flexural capacity of column M_n is:

$$P_n = C_c + \sum_{i=1}^n F_{s,i} \quad (8)$$

$$M_n = (C_c \bar{y}_c) + \sum_{i=1}^n (F_{s,i} \bar{y}_{s,i}) \quad (9)$$

where n , $\bar{y}_{i=1}$ and $\bar{y}_{s,i}$ are the number of bars at each

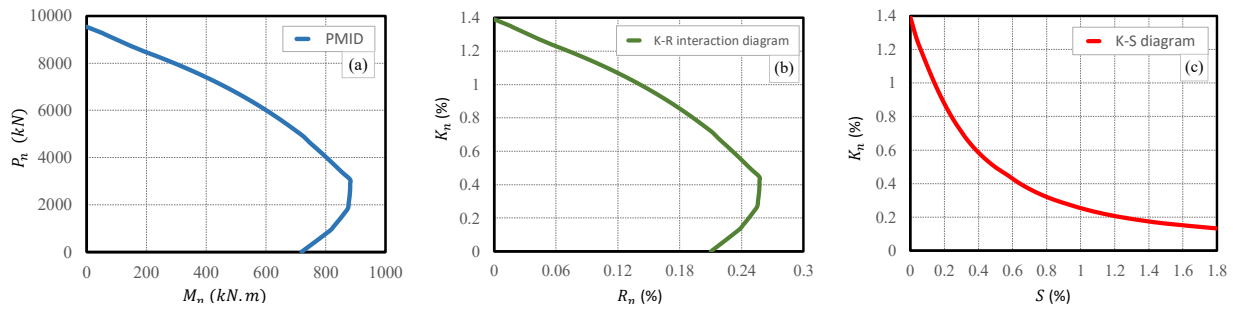


Fig. 4. Stepwise graphical process of transposing diagrams from (a) PMID to (b) $K_n \cdot R_n$ interaction diagram and then to (c) $K_n \cdot S$ diagram for a cross section with $h = b = 50 \text{ cm}$, $f'_c = 28 \text{ MPa}$, $f_y = 420 \text{ MPa}$, $\gamma = 0.8$ and 5 bars at each side ($\rho = 4\%$)

side, the distance between centroid of compressive zone of concrete and principal axis P.A, and the distance between i th row of bars and P.A, respectively.

4.2. Curve and Surface Fitting

Curve and Surface Fitting is a process of constructing a mathematical function which has the best fit to a given series of points. The Goodness of fit is an index which can be evaluated by some parameters including R-square, Adjusted R-Square, Root Mean Square Error (RMSE) and Sum of Square due to Error (SSE). "Curve Fitting" is an application which is provided in MATLAB and can fit appropriate curves in 2-dimensional coordinate system and surface in 3-dimensional coordinate system to data points. Although there are some default functions available with different features, but fitting process can be carried out according to custom equations.

5- METHOD DEVELOPMENT

As discussed above, for reaching desired PMID for a Case of cross section with specific options including PMID dimensions, f'_c , f_y , γ , and arrangement of bars, the four stages of theory procedure have to be carried out for different values of c . Here, it is done for 200 values of c in the interval $[0, h^2/10]$ where h is the height of cross section. In fact, this creates 200 loops of calculation in the modeling structure. Each one contains the theory procedure and the main idea of study. Some of the result points which fall into the fourth quarter of the derived PMIDs are neglected.

5.1. Description of Main Idea

As can be seen in Fig. 2, there are several slanted lines which cut the $K_n - R_n$ curves. Each line shows a unique value of

$$S = \frac{e}{h} \tag{10}$$

where

$$e = \frac{M}{P} \tag{11}$$

In the design procedure, P and M are considered as factored axial load P_n and bending moment M_n , respectively. But in this section of paper, these are defined as nominal capacities to reach probable eccentricities of the cross section. Since there is one unique point (M_n, P_n) for each c , so also there is a e for each c .

The dimensionless parameters

$$K_n = \frac{P_n}{f'_c A_g} \tag{12}$$

$$R_n = \frac{P_n e}{f'_c A_g h} \tag{13}$$

where $A_g = bh$ for square section and $A_g = \pi h_c^2/4$, establish the main design diagrams. In this paper, two parameters of K_n and S are considered as the major parameters. In other words, the provided formula for determining the percentage of reinforcement in cross section is a two-variable function of K_n and S . Since the column behavior is assessed in each integer percentage of ρ , 1% to 8%, the diameter of bars D considered in rectangular cross section is derived as:

$$D = \sqrt{\frac{4 \rho A_g}{\pi n_b}} \tag{14}$$

where n_b is the total number of bars in cross section. After determining P_n and M_n of each ρ of any case for 200 c , K_n and S are easily computed. Fig. 4 illustrates the main steps of transposing the diagrams for a case with $h = b = 50 \text{ cm}$, $f'_c = 28 \text{ MPa}$, $f_y = 420 \text{ MPa}$, $\gamma = 0.8$, $\rho = 4\%$, and 5 bars at each side.

5.2. Effectiveness Assessment of options

As can be figured out from Fig. 2, the dimension option is neglected in list of options of a case in means of dividing the capacity by h . It means that these diagrams are applicable for any desired dimension. But in spite of dividing the capacity by f'_c , it still remains as an option in each case. However,

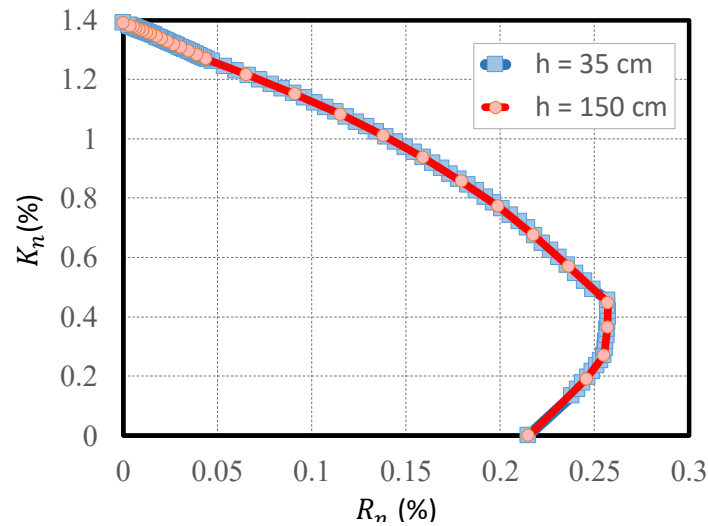


Fig. 5. Effect of dimension on the interaction diagram

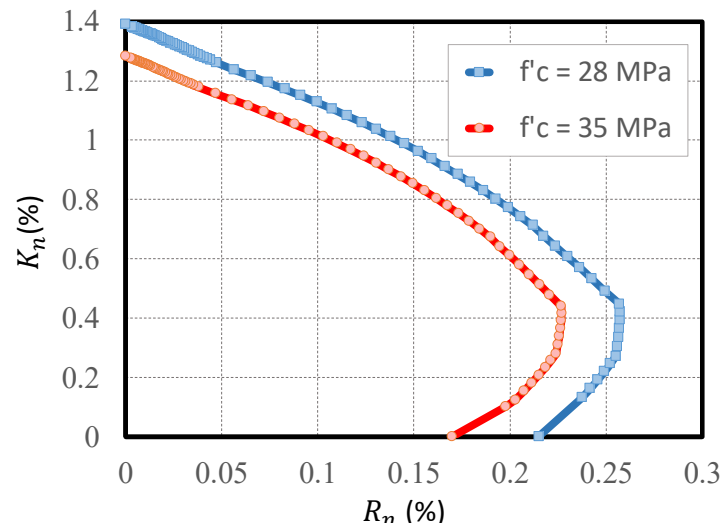


Fig. 6. Effect of compressive strength of concrete on the interaction diagram

detailed evaluation of effectiveness of each option on capacity values can be useful. This assessment is carried out from a comparison point of view according to $K_n - R_n$ interaction diagrams. It is clear that any effect on such diagrams is similar to $K_n - S$ diagrams which are the basis of the method. As the shape of cross section is an inevitable fixed option in a case, the effect of shape is not evaluated here.

5.2.1. Cross-Sectional Dimension

By assuming $f'_c = 28 \text{ MPa}$, $f_y = 420 \text{ MPa}$, $\gamma = 0.8$, $\rho = 4\%$ and 5 bars at each side, Fig. 5 shows the diagrams for two cross sections with a square shape of $h = b = 35 \text{ cm}$ and a rectangular cross section of $h = 150 \text{ cm}$ and $b = 50 \text{ cm}$. According to perfect match between data series of two cross sections, it is obvious that eliminating dimension from each case is reasonable. Also, this is shown that this method can be used for designing both RC columns and URSWs. This helps

the generalization of the method by which the value of ρ can be determined for any desired dimension. It is useful to mention that the shape of the column which considered as a lateral option of each case is latent in dimension option. For more assurance, in this paper, the dimensions of $h = b = 35 \text{ cm}$ and $h = b = 150 \text{ cm}$ are simultaneously studied for each case.

5.2.2. Compressive Strength of Concrete f'_c

It is clear from $K_n - R_n$ interaction design diagrams that f'_c is considered as an option in each case. The mismatch between data points shown in Fig. 6 proves this statement. The parameters $h = 50 \text{ cm}$, $f_y = 420 \text{ MPa}$, $\gamma = 0.8$, $\rho = 4\%$ and the arrangement of 5 bars at each side are considered for $f'_c = 28 \text{ MPa}$ and $f'_c = 35 \text{ MPa}$ in this comparison.

5.2.3. Tensile Strength of Steel f_y

It seems that f_y cannot be dismissed from the list of

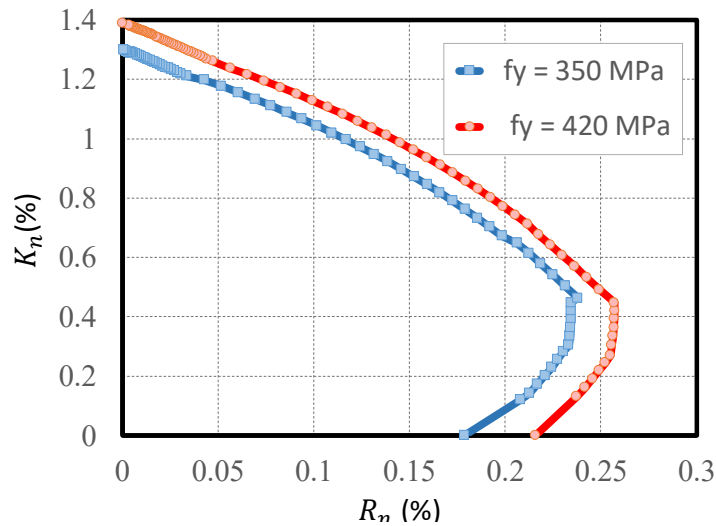


Fig. 7. Effect of tensile strength of stress on the interaction diagram

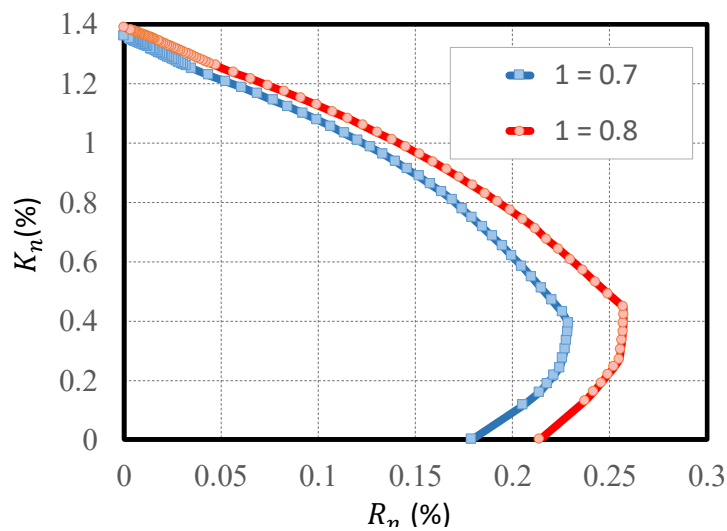


Fig. 8. Effect of parameter γ on the interaction diagram

option of a case, because this parameter does not cooperates in the task of dividing the capacity. For graphical proof, the interaction diagrams of a cross section with $h = b = 50\text{cm}$, $f'_c = 28\text{MPa}$, $\gamma = 0.8$, $\rho = 4\%$ and arrangement of 5 bars at each side for $f_y = 350\text{MPa}$ and $f_y = 420\text{MPa}$ are displayed in Fig. 7.

5.2.4. parameter γ

The behavior of two cross sections with $h = b = 50\text{cm}$, $f'_c = 28\text{MPa}$, $f_y = 420\text{MPa}$, $\rho = 4\%$ and 5 bars at each side for $\gamma = 0.7$ and $\gamma = 0.8$ is illustrated in Fig. 8. It shows that this parameter still remains as an option of each case.

5.2.5. Arrangement of Bars

The mismatch between two diagrams illustrated in Fig. 9 and corresponded to a cross section with $h = b = 50\text{cm}$

, $f'_c = 28\text{MPa}$, $f_y = 420\text{MPa}$, $\gamma = 0.8$, $\rho = 4\%$ for two arrangements of 4 and 5 bars at each side shows that the option of bars arrangement cannot be deleted from the list of options of a case.

5.3. Net Tensile Strain Evaluation

According to basic criteria $\phi P_n \leq P_u$ and considering equality between two sides of inequality in design procedure, by substituting, K_n turns to

$$K_n = \frac{P_u}{\phi f'_c A_g} \tag{15}$$

where ϕ is the strength reduction factor which, according to ACI, varies between 0.65 to 0.90. This factor is a function

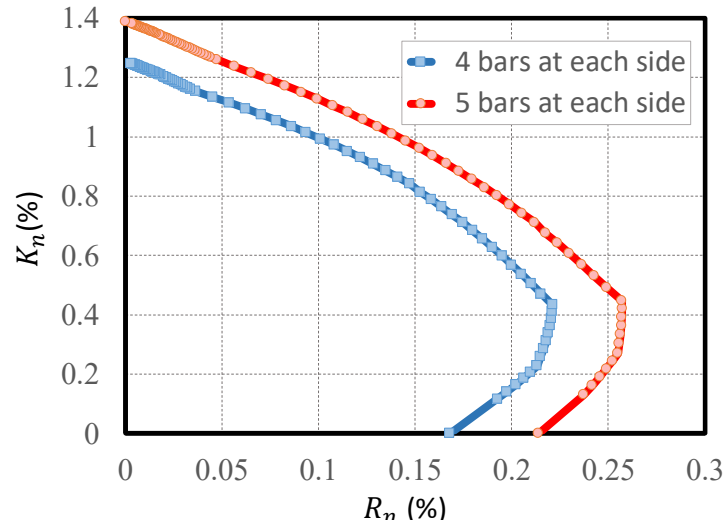


Fig. 9. Effect of bars arrangement on the interaction diagram

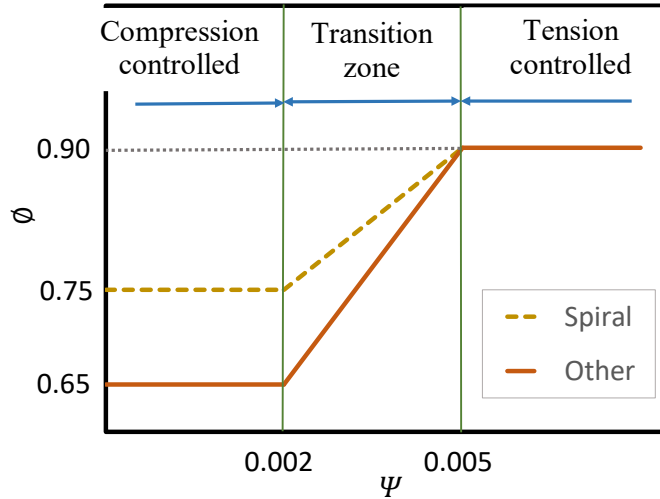


Fig. 10. Variation of ϕ with ψ

of net tensile strain ψ , which is defined as

$$\phi = \begin{cases} 0.75 & \text{for } \psi < 0.002 \\ 0.75 + (\psi - 0.002)50 & \text{for } 0.002 \leq \psi \leq 0.005 \\ 0.90 & \text{for } \psi > 0.005 \end{cases} \quad (16)$$

for spirally reinforced columns and

$$\phi = \begin{cases} 0.65 & \text{for } \psi < 0.002 \\ 0.65 + (\psi - 0.002)(250/3) & \text{for } 0.002 \leq \psi \leq 0.005 \\ 0.90 & \text{for } \psi > 0.005 \end{cases} \quad (17)$$

for other types of reinforcement. In another words, the value of this factor depends on the establishment zone of last row of bars including compression-controlled, transition

and tension-controlled zone. Fig. 10 shows the variation of strength reduction factor with net tensile strain in the last row of steel bars for spirally and other reinforced columns. Therefore, it is become important to evaluate the behavior of this row of bars from a strain point of view. The strain values versus S and K_n in a case with $h = b = 50\text{ cm}$, $f'_c = 28\text{ MPa}$, $f_y = 420\text{ MPa}$, $\gamma = 0.8$, $\rho = 4\%$ and 5 bars at each side are illustrated in Fig. 11 and Fig. 12, respectively.

6- CURVE AND SURFACE FITTING AND FORMULATION

After determining 400 values of each desired dimensionless parameter, K_n and S , for eight ρ in each case and then neglecting negative values, fitting process has to be done. A 2D fitting is used to establish the formula $K_n = f(S)$ for each

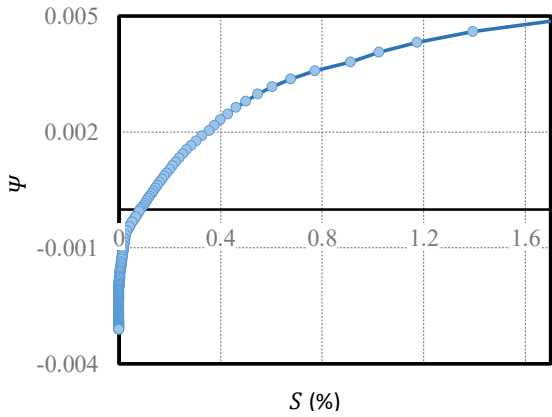


Fig. 11. Ψ - S in a case with a circular cross section, $f'_c = 28 \text{ MPa}$, $f_y = 420 \text{ MPa}$, $\gamma = 0.8$, $\rho = 4\%$ and 5 bars at each side

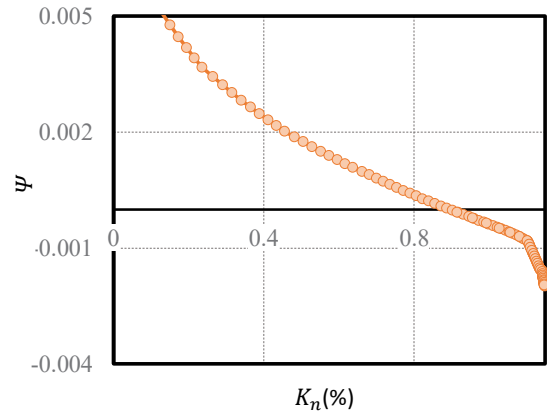


Fig. 12. Ψ - K_n in a case with a circular cross section, $f'_c = 28 \text{ MPa}$, $f_y = 420 \text{ MPa}$, $\gamma = 0.8$, $\rho = 4\%$ and 5 bars at each side

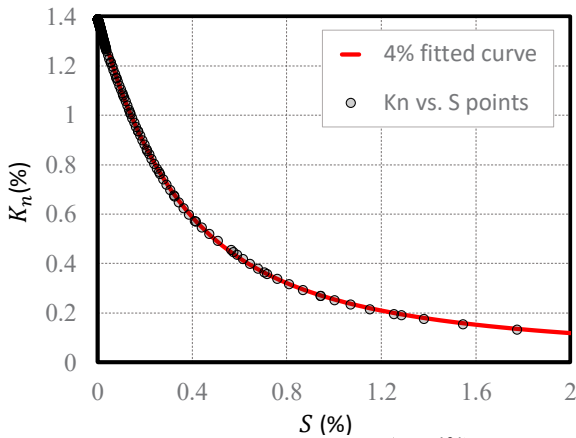


Fig. 13. Data points and fitted curve for $\rho = 4\%$ of a case with rectangular cross section, $f'_c = 28 \text{ MPa}$, $f_y = 420 \text{ MPa}$, $\gamma = 0.8$ and 5 bars at each side.

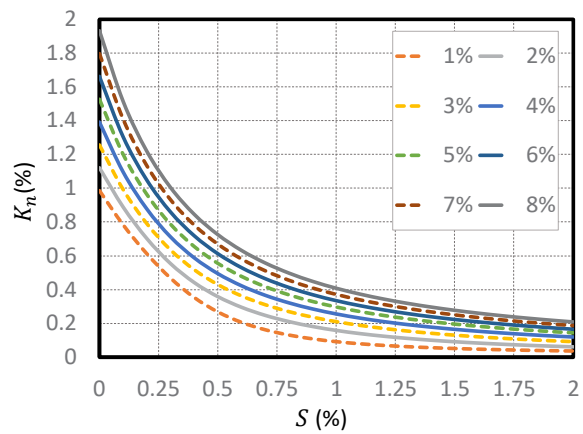


Fig. 14. K_n and S diagram of a case with rectangular cross section, $f'_c = 28 \text{ MPa}$, $f_y = 420 \text{ MPa}$, $\gamma = 0.8$ and 5 bars at each side

ρ . The type of 2D fitting used is a built-in type in Curve Fitting App named Rational in which the numerator and denominator degrees are selected 2 and 3, respectively. The general model used in this type is defined as:

$$f(x) = \frac{p_1 x^2 + p_2 x + p_3}{x^3 + q_1 x^2 + q_2 x + q_3} \quad (18)$$

where p_1 to p_3 and q_1 to q_3 are the coefficients whose determination is the main objective of fitting process. It should be noted that $f(x)$ and x are related to K_n and S , respectively. As the 2D fitting is carried out only for preparing data for 3D fitting, the number of coefficients does not play an important role. But the values which describe the goodness of fitting are considerable, because they affect the accuracy of method. Fig. 13 shows the data points and fitted curve for $\rho = 4\%$ of a case with rectangular cross section, $f'_c = 28 \text{ MPa}$, $f_y = 420 \text{ MPa}$, $\gamma = 0.8$ and 5 bars at each side.

By doing this for eight ρ of a case, K_n - S diagram of this case is derived which can be seen in Fig. 14. To represent the accuracy of fitting and the selecting the type, the values of goodness of fitting for each ρ of this case is listed in Table 1. When the value of R^2 which varies in the interval $[-\infty, 1]$ is calculated equal to 1 in the fitting process, it means that the curve or surface perfectly fitted the data set of points.

The data points for 3D fitting of calculating ρ are generating based on this 2D formulation, so that the average value of R^2 of 2D fitting for eight ρ in each case is applied to the accuracy of final formulation of ρ .

6.1. Formulation of ρ

To present the main formula $\rho = f(K_n, S)$, a series of data point is needed. After applying 40 points in the interval $[0, 2]$ of S at the $K_n = f(S)$ for each eight ρ , which is derived from the 2D fitting, the data points for eight ρ at each case are available. These sets of data are used for 3D fitting in which a Polynomial type of fitting is considered. The Eq. 19 and 20

Table 1. Values of goodness of fitting performed in Fig. 13

	1%	2%	3%	4%	5%	6%	7%	8%
R^2	1	1	1	1	1	1	1	1
RMSE	0.001374	0.001475	0.00157	0.001722	0.001845	0.00193	0.001991	0.002027

Table 2. A comparison between the best possible models for obtaining ρ in rectangular cross sections

Mathematical Model of $f(x,y)$	Num. of Coefficients	R^2	RMSE
$u_1 + u_2x + u_3xy$	3	0.7064	1.2470
$u_1 + u_2y + u_3xy$	3	0.9057	0.7069
$u_1 + u_2x^2 + u_3xy$	3	0.6713	1.3200
$u_1 + u_2y^2 + u_3xy$	3	0.9696	0.4016
$u_1 + u_2x^2 + u_3y + u_4xy$	4	0.9554	0.4871
$u_1 + u_2x + u_3y^2 + u_4xy$	4	0.9859	0.2736
$u_1 + u_2x + u_3x^2 + u_4y^2 + u_5xy$	5	0.9869	0.2648
$u_1 + u_2x^2 + u_3y + u_4y^2 + u_5xy$	5	0.9842	0.2904

Table 3. A comparison between the best possible models for obtaining ρ in circular cross sections

Mathematical Model of $f(x,y)$	Num. of Coefficients	R^2	RMSE
$u_1 + u_2x + u_3xy$	3	0.6701	1.3220
$u_1 + u_2y + u_3xy$	3	0.7872	1.0620
$u_1 + u_2x^2 + u_3xy$	3	0.6662	1.3300
$u_1 + u_2y^2 + u_3xy$	3	0.8692	0.8325
$u_1 + u_2x^2 + u_3y + u_4xy$	4	0.8639	0.8506
$u_1 + u_2x + u_3y^2 + u_4xy$	4	0.9488	0.5215
$u_1 + u_2x + u_3x^2 + u_4y^2 + u_5xy$	5	0.9744	0.3693
$u_1 + u_2x^2 + u_3y + u_4y^2 + u_5xy$	5	0.9684	0.4105

Table 4. Results of the surface fitting shown in Fig. 15

u_1	u_2	u_3	u_4	R^2
-2.094	0.6277	2.968	21.33	0.9859

shows the general mathematical models which are defined for cases with rectangular and circular cross section, respectively.

$$f(x,y) = u_1 + u_2x + u_3y^2 + u_4xy \tag{19}$$

$$f(x,y) = u_1 + u_2x + u_3x^2 + u_4y^2 + u_5xy \tag{20}$$

The coefficients u_1 to u_5 are the main goal which should be calculated. The variables x , y and $f(x,y)$ represent S , K_n and ρ , respectively. The selection of these models is carried out according to: (1) less coefficients to make the design procedure simpler, (2) higher R^2 to improve the accuracy of method. A numerical comparison among the best possible models is provided in Table 2 for rectangular cross section and in Table 3 for circular cross section. Also,

the value of RMSE for each model is listed in the tables for more information. These comparisons are performed based on $f'_c = 28\text{MPa}$, $f_y = 420\text{MPa}$, $\gamma = 0.8$ and 5 bars at each side of rectangular cross section and total 8 bars at the circular cross section. However, the 3D visualization of the data points and final fitted surface is shown in Fig. 15. Finally, the results of the fitting shown in Fig. 15 are listed in Table 4. It is important to say that the output of the proposed formula for ρ is calculated in percentage, so that this derived value has to be divided by 100.

6.2. Formulation of strength reduction factor ϕ

The straight lines which define the values of $\Psi = 0.002$ and $\Psi = 0.005$ in design aid diagrams provided in [24] are slanted. Also, illustrating the variation of Ψ with K_n and S in Fig. 10 and Fig. 11, respectively, proves this fact. However,

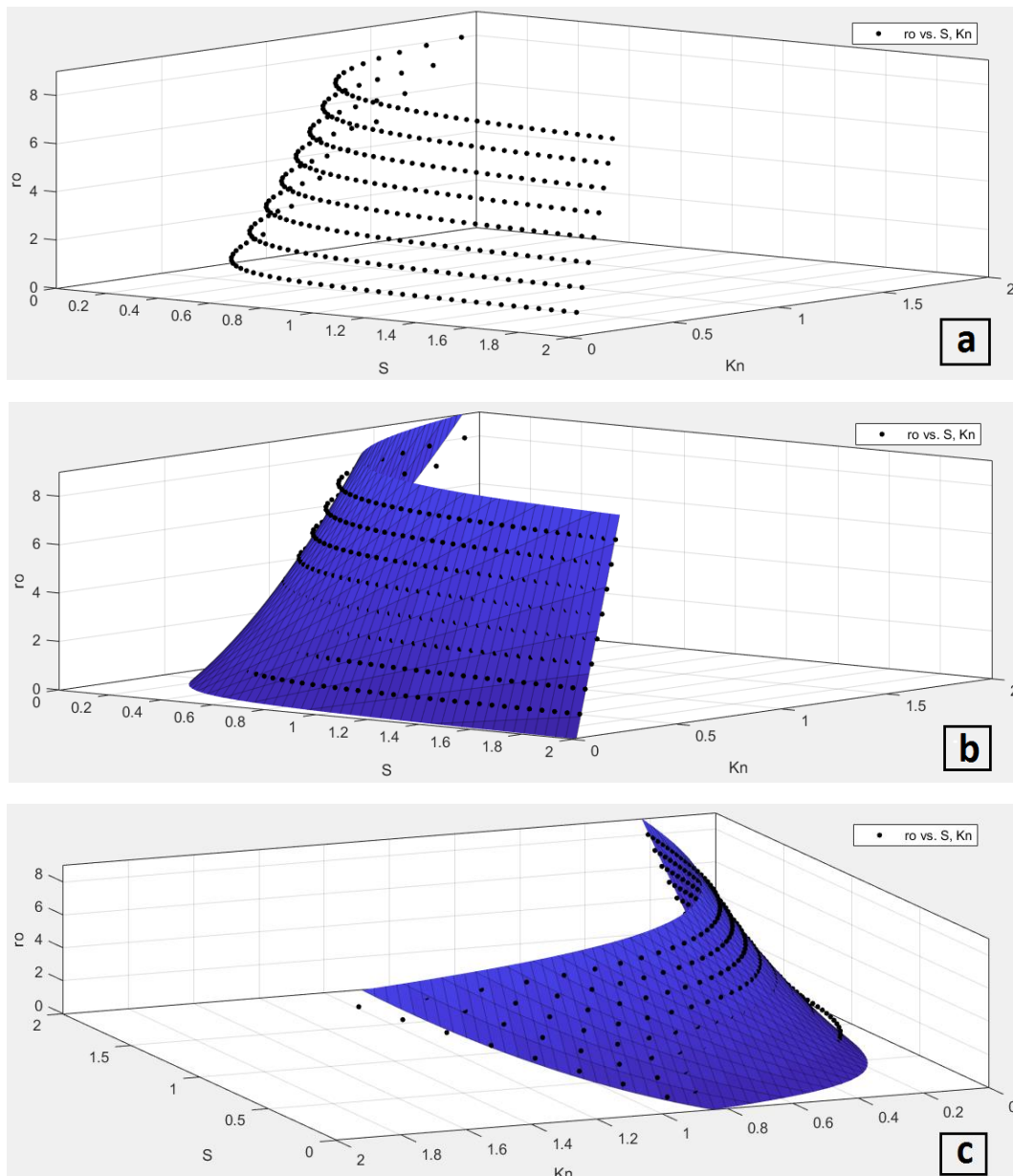


Fig. 15. 3D visualization of: (a) data points, (b) view1 of fitted surface, and (c) view2 of fitted surface, according to selected general model of obtaining ρ , for a case with rectangular cross section, $f'_c = 28 \text{ MPa}$, $f_y = 420 \text{ MPa}$, $\gamma = 0.8$, and 5 bars at each side

by applying Eq. 16 or Eq. 17 to the calculated and gathered vectors of Ψ for eight ρ of a case, 3D visualization of data points for ρ versus K_n and S is derived which is shown in Fig. 16 for a case with rectangular cross section, $f'_c = 28 \text{ MPa}$, $f_y = 420 \text{ MPa}$, $\gamma = 0.8$, and 5 bars at each side. The behavior of strength reductant factor versus K_n and S shows that the value of ρ can be approximately considered only as a function of K_n with neglecting the variation of this factor with S . This is because the data points (Ψ, K_n, S) or (ρ, K_n, S) does not show a good behavior for surface fitting with high accuracy. Therefore, the formulation is performed based on linear interpolation for bounds of K_n in the interval $[K_n^{\rho=0.90}, K_n^{\rho=0.75}]$ for spiral reinforcement and $[K_n^{\rho=0.90}, K_n^{\rho=0.65}]$

for other types of reinforcement. The final results of the case mentioned above is listed in Table 5.

7- RESULTS PRESENTATION

The described procedure for proposing the FbD method is carried out for some cases with commonly used options. The final results for process of determining ρ and ρ using FbD method are provided in Table 6 to Table 8. The considered mathematical models which is compatible for all of the cases in the corresponding table is provided. Instead of using design diagrams, these Tables of FbD method can be used for design of eccentrically loaded columns and URSWs considering the common strength and geometric parameters.

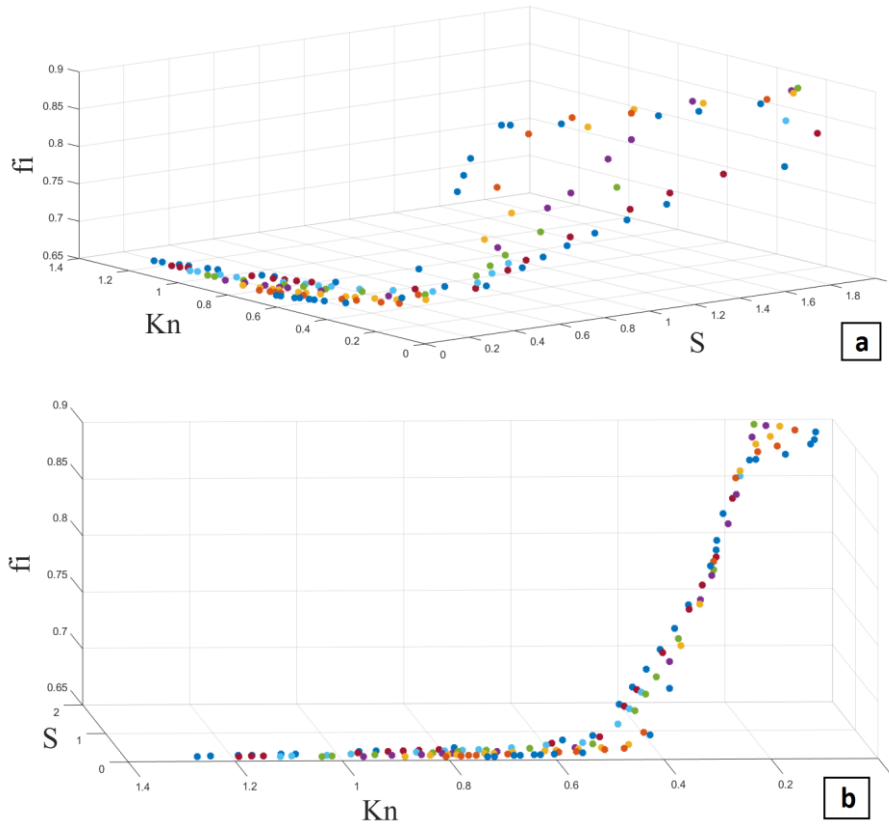


Fig. 16. 3D visualization of data points for ϕ versus S and K_n for a case with rectangular cross section, $f'_c = 28 \text{ MPa}$, $f_y = 420 \text{ MPa}$, $\gamma = 0.8$, and 5 bars at each side, (a) view1, and (b) view2

Table 5. Results for obtaining ϕ in the case of Fig. 16

Bounds of K_n	Value of ϕ
$0.4532 \leq K_n$	0.65
$0.1103 < K_n < 0.4532$	$0.65 + (0.4532 - K_n) 0.6660$
$0.1103 \geq K_n$	0.90

Since several load combinations are considered in designing procedure and the maximum value of ρ among the derived values is selected as the final result, using this method decreases the complexity and time of this procedure. For a given factored load P_u and factored bending moment M_u , the following steps using FbD method are proposed for designing columns and URSWs:

1. Calculate eccentricity $e = M_u / P_u$.
2. Select trial cross-sectional dimensions b and h for URSWs and rectangular and h_c for circular cross section.
3. Assume a trial $\phi = 0.65$ and calculate $K_n = P_u / \phi f'_c A_g$ and $S = e / h$.
4. Calculate $\phi = f(K_n)$ according to corresponding table and check if the trial assumption is correct; otherwise, calculate K_n with derived ϕ .

5. Calculate $\rho = f(S, K_n)$ according to corresponding table.

6. Calculate total steel reinforcement area $A_{st} = \rho bh / 100$.

According to the effectiveness assessments, proposed values in these tables are only applicable for mentioned related options. Fig. 17 shows the flowchart of the whole process of obtaining the formulas for designing RC column and URSW, which can be used for providing the required values of desired options.

Note that according to the part of the proposed tables which is dedicated to the ϕ , the values of the both bounds $K_n^{\phi=0.90}$ and $K_n^{\phi=0.75}$ increase with the increase in γ for specific f'_c and f_y , and this happens for values of ω vice versa.

8- METHOD VALIDATION AND ACCURACY

It is obvious that FbD method can make the hand design

Table 6. FbD method for Rectangular cross section and 5 bars at each side

Short RC Columns and Uniformly Reinforced Shear Walls													
<ul style="list-style-type: none"> Rectangular Cross Section 5 Bars at Each Side of Cross Section Non-spirally Reinforcement 													
Case	Option f'_c and f_y in MPa			$\rho^{rectangular} = u_1 + u_2S + u_3K_n^2 + u_4SK_n$ $e = \frac{M_u}{P_u}$, $S = \frac{e}{h}$, $K_n = \frac{P_u}{\phi f_y A_g}$					$\phi = 0.65$ $K_n^{\phi=0.65} \leq$ $\phi = 0.65 + (K_n^{\phi=0.65} - K_n) \omega$ $K_n^{\phi=0.90} <$ $\phi = 0.90$ $K_n^{\phi=0.90} \geq$				
	f'_c	f_y	γ	u_1	u_2	u_3	u_4	u_5	R^2	$K_n^{\phi=0.65}$	$K_n^{\phi=0.90}$	ω	
1	2 8	420	0.6	-2.380	0.610	3.366	29.67	-	0.968 1	0.3673	0.0796	0.8690	
2	2 8	420	0.7	-2.144	0.561	3.129	24.85	-	0.976 1	0.3748	0.0989	0.9061	
3	2 8	420	0.8	-2.094	0.628	2.968	21.33	-	0.985 2	0.4089	0.1103	0.8372	
4	2 8	420	0.9	-1.778	0.494	2.707	18.09	-	0.987 5	0.4532	0.1151	0.7394	
5	3 5	420	0.6	-2.872	1.022	4.252	34.38	-	0.957 1	0.3623	0.0986	0.9480	
6	3 5	420	0.7	-2.630	0.950	4.022	28.98	-	0.970 3	0.3932	0.1095	0.8811	
7	3 5	420	0.8	-2.570	1.003	3.860	25.03	-	0.982 1	0.4474	0.1059	0.7322	
8	3 5	420	0.9	-2.455	0.926	3.643	21.93	-	0.988 1	0.4837	0.1301	0.7070	

Table 7. FbD method for Rectangular cross section and 4 bars at each side

Short RC Columns and Uniformly Reinforced Shear Walls													
<ul style="list-style-type: none"> Rectangular Cross Section 4 Bars at Each Side of Cross Section Non-spirally Reinforcement 													
Case	Option f'_c and f_y in MPa			$\rho^{rectangular} = u_1 + u_2S + u_3K_n^2 + u_4SK_n$ $e = \frac{M_u}{P_u}$, $S = \frac{e}{h}$, $K_n = \frac{P_u}{\phi f_y A_g}$					$\phi = 0.65$ $K_n^{\phi=0.65} \leq$ $\phi = 0.65 + (K_n^{\phi=0.65} - K_n) \omega$ $K_n^{\phi=0.90} <$ $\phi = 0.90$ $K_n^{\phi=0.90} \geq$				
	f'_c	f_y	γ	u_1	u_2	u_3	u_4	u_5	R^2	$K_n^{\phi=0.65}$	$K_n^{\phi=0.90}$	ω	
1	2 8	420	0.6	-2.958	1.015	4.465	35.77	-	0.955 8	0.3668	0.0937	0.9154	
2	2 8	420	0.7	-2.656	0.978	4.225	29.76	-	0.966 4	0.3993	0.1043	0.8473	
3	2 8	420	0.8	-2.583	1.015	4.055	25.80	-	0.978 7	0.4454	0.1121	0.7501	
4	2 8	420	0.9	-2.526	0.998	3.865	22.71	-	0.987 2	0.4766	0.1146	0.6904	
5	3 5	420	0.6	-3.465	1.502	5.385	41.15	-	0.936 7	0.3666	0.1037	0.9509	
6	3 5	420	0.7	-3.262	1.486	5.21	35.08	-	0.953 5	0.3979	0.1067	0.8586	
7	3 5	420	0.8	-3.152	1.394	5.018	30.77	-	0.972 4	0.4362	0.1126	0.7727	
8	3 5	420	0.9	-3.037	1.358	4.807	27.03	-	0.981 2	0.4692	0.1258	0.7279	

Table 8. FbD method for Circular cross section and 8 total bars at cross section

Short RC Columns															
<ul style="list-style-type: none"> • Circular Cross Section • 8 total Bars at Cross Section • Spirally Reinforcement 															
Case	Options f'_c and f_y in MPa			$\rho^{circular} = u_1 + u_2S + u_3S^2 + u_4K_n^2 + u_5SK_n$ $e = \frac{M_u}{P_u}$, $S = \frac{e}{h}$, $K_n = \frac{P_u}{\phi f_y A_g}$						$\phi = 0.75$	$K_n^{\phi=0.75} \leq$	$\phi = 0.75 + (K_n^{\phi=0.65} - K_n) \omega$	$K_n^{\phi=0.90} <$	$\phi = 0.90$	$K_n^{\phi=0.90} \geq$
	f'_c	f_y	γ	u_1	u_2	u_3	u_4	u_5	R^2	$K_n^{\phi=0.65}$	$K_n^{\phi=0.90}$	ω			
1	28	420	0.6	-5.980	8.491	-3.85	7.019	57.24	0.8802	0.9075	0.0314	0.1712			
2	28	420	0.7	-5.874	5.339	-1.669	6.840	57.60	0.9308	0.3996	0.0504	0.4296			
3	28	420	0.8	-5.343	5.117	-1.625	6.575	49.97	0.9744	0.4554	0.0702	0.3893			
4	28	420	0.9	-5.242	5.153	-1.617	6.541	45.35	0.9836	0.4942	0.0906	0.3716			
5	35	420	0.6	-6.948	6.920	-2.239	8.417	71.47	0.9410	0.8442	0.0272	0.1836			
6	35	420	0.7	-6.41	6.596	-2.129	8.142	62.72	0.9532	0.3921	0.0739	0.4713			
7	35	420	0.8	-6.394	6.667	-2.127	8.183	57.83	0.9682	0.4522	0.1032	0.4297			
8	35	420	0.9	-6.327	6.675	-2.113	8.175	53.24	0.9772	0.5025	0.0967	0.3696			

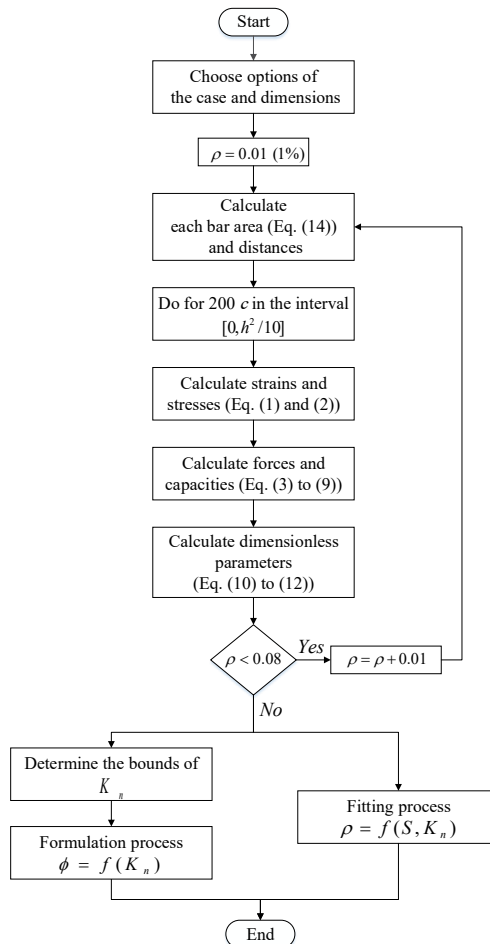


Fig. 17. Flowchart of overall process of deriving formulas

Table 9. Assessment of method accuracy according to R^2 values

	Table 6		Table 7		Table 8		All tables	
	Mean Value	Maximum	Mean Value	Maximum	Mean Value	Maximum	Mean Value	Maximum
R^2 value	0.9768	0.9881	0.9665	0.9872	0.9511	0.9836	0.9648	0.9881
Case Number	-	8	-	4	-	4	-	8 (Table 6)

Table 10. Results of Example

Dimensions cm×cm (in×in)	S	K_n	FbD Method		Design interaction diagrams		Error (%)
			\emptyset	ρ [%]	\emptyset	ρ [%]	
45×45 (17.7×17.7)	0.3333	0.8683	0.65	6.5260	0.65	6.55	-0.37
50×50 (19.7×19.7)	0.3000	0.7033	0.65	4.0629	0.65	4	+1.57
55×55 (21.7×21.7)	0.2727	0.5812	0.65	2.4605	0.65	2.35	+4.70

steps faster and easier by using provided formulas, but it is important to assess the accuracy of the method, and to validate the method. The validation is carried out through an example in which the results derived from FbD method are compared to the results of the other common method, i.e. using design interaction diagrams.

8.1. Method Accuracy

The value of R^2 which is the main component of goodness of fitting parameters is used to evaluate the accuracy of method. Table 9 presented a brief assessment of three proposed tables according to R^2 values. It can be figured out from this table that the best results are achieved for Case 8 of Table 6 which corresponds to the rectangular cross section with 5 bars at each side. This case has the minimum error of 1.19%, and the maximum error of 11.98% relates to the Case 1 of Table 8 with $R^2 = 0.8802$. Also, for specific f'_c and f_y , the value of R^2 increases with increment of γ .

Since the linear interpolation for formulation of \emptyset is performed based on the bounds of $[K_n^{\emptyset=0.90}, K_n^{\emptyset=0.75}]$ or $[K_n^{\emptyset=0.90}, K_n^{\emptyset=0.65}]$, depending on the type of reinforcement, the R^2 value of this linear fitting is equal to 1 for all of the cases.

8.2. Example

A rectangular cross section with 5 bars at each side, $f'_c = 28 MPa$ (4 ksi), $f_y = 420 MPa$ (60 ksi), $\gamma = 0.8$ which is subjected to $P_u = 3200$ kN (719.3 kips) and $M_u = 480$ kN.m (353.7 kips.ft) is assumed. Calculate the value of ρ for common used dimensions of cross section.

8-2-1. Solution

First of all, $e = 15$ cm. Using Case 3 in Table 6 and mentioned steps, the solution continues in the Table 10. Also, the visual inspection results from the design interaction diagram in [24] are provided to make a comparison between two methods.

9- CONCLUSIONS

In this paper, a straightforward Formula-based Design method is proposed by which the values of ρ and \emptyset can

be calculated. According to several assessments carried out through the research and the derived results, it can be concluded that:

- The FbD method is applicable for designing columns and uniformly reinforced shear walls.
- Derived values using this method are the exact required amounts in design procedure.
- This method permits a faster and direct design in hand calculations.
- Well-organized formulas are useful for direct modeling of standard shapes of column in different research fields, such as reliability and probabilistic studies.
- Considering the common strength and geometric options for each case is reasonable.
- The idea of using fitting technique is responsive to the final goals of this paper, and can be used for generating more results for any required option.
- The effect of slenderness is not considered in this method, and may be taken into account in a future study.

NOMENCLATURE

- a height of stress block of concrete compression zone
- A_c area of concrete compression zone
- A_g cross section gross area
- b width of cross section
- c distance from fiber of maximum compressive strain to neutral axis
- C_c force in concrete compression zone
- d_i distance from the fiber of maximum compressive strain to centroid of i th row of bars
- D diameter of bar
- e eccentricity
- E_s elastic modulus of steel
- f'_c compressive strength of concrete
- f_{si} stress in i th row of bars
- F_{si} force in i th row of bars
- f_y yield strength of steel
- h height of cross section

h_c diameter of circular cross section
 K_n dimensionless parameter corresponding to axial capacity
 $K_n^{\varnothing=0.65}$ bound of $\varnothing = 0.65$
 $K_n^{\varnothing=0.75}$ bound of $\varnothing = 0.75$
 $K_n^{\varnothing=0.90}$ bound of $\varnothing = 0.90$
 M_u factored bending moment
 M_n nominal flexural capacity
 N.A neutral axis
 n_b total number of bars at cross section
 P.A principal axis
 $p_1 \cdot p_2 \cdot p_3$ numerator coefficients of numerator in 2D fitting
 P_u factored load
 P_n nominal axial capacity
 $q_1 \cdot q_2 \cdot q_3$ denominator coefficients of denominator in 2D fitting
 R_n dimensionless parameter corresponding to flexural capacity
 S eccentricity to height of cross section
 $u_1 \cdot u_2 \cdot u_3 \cdot u_4 \cdot u_5$ coefficient of polynomial 3D fitting
 \bar{y}_c distance from centroid of concrete compression zone to principal axis
 γ distance between first and last row of bars to height of cross section ratio
 ρ reinforcement area to cross section gross area ratio
 \varnothing strength reduction factor
 Ψ net tensile strain
 θ angle in circular cross section which determine the compression zone
 ε_{cu} maximum compressive strain of concrete
 ε_{si} strain in i th row of bars

REFERENCES

- [1] J.K. Wight, J.G. MacGregor, Reinforced Concrete Mechanics and Design, 6th edition, Pearson Education, Inc., Upper Saddle River, New Jersey, 2012 (1157 pp)
- [2] B. Bresler, Design criteria for reinforced columns under axial load and biaxial bending, ACIS J. Proc. 57 (11) (1960) 481–490
- [3] K.H. Chu, A. Pabarcus, Biaxially loaded reinforced concrete columns, J. Struct. Div. ASCE 84 (ST8) (1958) 1–27.
- [4] C.S. Whitney, Plastic theory of reinforced concrete design, ASCE Trans. 107 (1942) (251 pp).
- [5] C.T. Hsu, M.S. Mirza, Structural concrete—biaxial bending and compression, J. Struct. Div. ASCE 99 (ST2) (1973) 285–290.
- [6] C.T.T. Hsu, Analysis and design of square and rectangular columns by equation of failure surface, ACI Struct. J. 85 (2) (1988) 167–179.
- [7] J.F. Fleming, S.D. Werner, Design of columns subjected to biaxial bending, ACI J. Proc. 62 (3) (1965) 327–342.
- [8] J. Marin, Design aids for L-shaped reinforced concrete columns, ACI J. (1979) 1197–1216 (Title No. 76-49).
- [9] C.T.T. Hsu, Biaxially loaded L-shaped reinforced concrete columns, J. Struct. Eng. ASCE 111 (12) (1985) 2576–2595.
- [10] C.T.T. Hsu, T-shaped reinforced concrete members under biaxial bending and axial compression, ACI Struct. J. 86 (4) (1989) 460–468.
- [11] C.I. Dinsmore, Column analysis with a programmable calculator, ACI Concr. Int. 4 (11)(1982) 32–36.
- [12] T. Brondum-Nielsen, Ultimate flexural capacity of partially or fully prestressed cracked arbitrary concrete sections under axial load combined with biaxial bending, ACI Concr. Int. 5 (1) (1983) 75–78.
- [13] J.R. Yen, Quasi-Newton method for reinforced concrete column analysis and design, J. Struct. Eng. ASCE 117 (3) (1991) 657–666.
- [14] J.L. Bonet, P.F. Miguel, M.A. Fernandez, M.L. Romero, Analytical approach to failure surfaces in reinforced concrete sections subjected to axial loads and biaxial bending, J. Struct. Eng. ASCE 130 (2004).
- [15] P. Paultre, F. Légeron, Confinement reinforcement design for reinforced concrete columns, J. Struct. Eng. ASCE 134 (5) (2008).
- [16] F. Barzegar, T. Erasito, Concrete sections under biaxial bending: interactive analysis with spreadsheets, ACI Concr. Int. 17 (12) (1995) 28–33.
- [17] H. Rodrigues, H. Varum, A. Arède, A.G. Costa, Behaviour of reinforced concrete column under biaxial cyclic loading—state of the art, Int. J. Adv. Struct. Eng. (IJASE) (2013).
- [18] A.Z. Zenon, W. Long, M.S. Troitsky, Designing reinforced concrete short-tied columns using the optimization technique, ACI Struct. J. 92 (5) (1995) 619–626.
- [19] R.D. Lequesne, J.A. Pincheira, Proposed revisions to the strength reduction factor for axially loaded members, ACI Concr. Int. 36 (9) (2014) 43–49.
- [20] W. Wang, H.P. Hong, Appraisal of reciprocal load method for reinforced concrete columns of normal and high strength concrete, J. Struct. Eng. ASCE 128 (11) (2002) 1480–1486.
- [21] J.A. Rodriguez, J.D. Aristizabal-Ochoa, Biaxial interaction diagram for short RC columns of any cross section, J. Struct. Eng. ASCE 125 (6) (1999).
- [22] L. Cedolin, G. Cusatis, S. Eccheli, M. Roveda, Biaxial bending of concrete columns: an analytical solution, Stud. Res. – Politec. di Milano 26 (2006) 163–192.
- [23] M. Mahamid, M. Houshiar, Direct design method and design diagrams for reinforced concrete columns and shear walls, J. Building Eng. 18 (2018) 66–75.
- [24] A. H. Nilson, D Darwin, C. W. Dolan, Design of Concrete Structures, 14th edition, McGraw-Hill, Inc.,
- [25] ACI 318-14, Building Code Requirements for Structural Concrete and Commentary.

HOW TO CITE THIS ARTICLE

J. Shafaei, R. Eskandari, Proposing Formula-Based Design Method for RC Columns and Uniformly Reinforced Shear Walls, AUT J. Civil Eng., 4(2) (2020) 249-264.

DOI: [10.22060/ajce.2019.15753.5548](https://doi.org/10.22060/ajce.2019.15753.5548)

